frontiers in Materials

ORIGINAL RESEARCH
published: 26 November 2020
doi: 10.3389/fmats.2020.600887

Photodegradation Kinetics of Alkyd Paints: The Influence of Varying Amounts of Inorganic Pigments on the Stability of the Synthetic Binder

Laura Pagnin[1], Rosalba Calvini[2], Rita Wiesinger[1], Johannes Weber[3] and Manfred Schreiner[1,4]*

[1]Institute of Natural Sciences and Technology in the Arts, Academy of Fine Arts, Vienna, Austria, [2]Department of Life Sciences, University of Modena and Reggio Emilia, Reggio Emilia, Italy, [3]Institute of Conservation Sciences, University of Applied Arts Vienna, Vienna, Austria, [4]Institute of Chemical Technologies and Analytics, Vienna University of Technology, Vienna, Austria

OPEN ACCESS

Edited by:
Enrico Sassoni, University of Bologna, Italy

Reviewed by:
Elisabetta Zendri, Ca' Foscari University of Venice, Italy
Massimo Lazzari, University of Santiago de Compostela, Spain

***Correspondence:**
Laura Pagnin
l.pagnin@akbild.ac.at

Specialty section:
This article was submitted to Environmental Materials, a section of the journal Frontiers in Materials

Received: *31 August 2020*
Accepted: *6 November 2020*
Published: *26 November 2020*

Citation:
Pagnin L, Calvini R, Wiesinger R, Weber J and Schreiner M (2020) Photodegradation Kinetics of Alkyd Paints: The Influence of Varying Amounts of Inorganic Pigments on the Stability of the Synthetic Binder. Front. Mater. 7:600887. doi: 10.3389/fmats.2020.600887

As the effects of climate change pose an increasing risk of damaging outdoor modern and contemporary artworks' aesthetic appearance by affecting their mechanical properties and chemical-physical stability, understanding the degradation processes attacking these objects is becoming more and more essential to their conservation. For this purpose, the kinetics of photo-oxidation processes occurring in alkyd paints and their stability in mixtures with different inorganic pigments were investigated. The aim was to characterize the different degradation reactions over time and study the photodegradation kinetics according to different pigments and pigment/binder ratios. This paper describes the degradation behavior of artificial ultramarine blue, hydrated chromium oxide green, and cadmium sulfate yellow pigments mixed with alkyd resin and aged under simulated sunlight exposure for a total of 1,008 h. The analytical techniques used offer complementary information on the characterization of the samples and their aging. Specifically, 3D Optical Microscopy allowed studying morphological and color changes. These results were supported by Scanning Electron Microscopy and Colorimetry analyses, also focused on studying the physical and granulometric characteristics of the pigments in relation to the binder degradation. Finally, qualitative and quantitative analysis was performed by Attenuated Total Reflection Infrared Spectroscopy. To support the obtained results, Multivariate Analysis of microscopic images was carried out with the aim of studying the degradation effects linked to color and texture changes. The obtained results demonstrate that the degradation processes of alkyd resin are influenced by the presence of the different inorganic pigments used and their concentration in the mixtures. This study should contribute as support to the field of conservation-restoration to find suitable protection strategies for paint surfaces against degradation agents.

Keywords: alkyd resin, photodegradation, inorganic pigments, multivariate analysis, infrared spectroscopy, scanning electron microscopy, colorimetry

INTRODUCTION

With the development of synthetic organic chemistry at the beginning of the 20th century, contemporary artists started to use a significant number of new polymeric materials as paint binders for creating artworks. Consequently, gathering knowledge related to proper preservation techniques for these artworks has become increasingly important on the international level (Chiantore and Rava, 2005). Several polymeric structural changes lead to mechanical properties and chemical stability modifications which eventually result in and degradation of the binder (Rosu and Visakh, 2016). Early studies (Rabek, 1995; Learner, 2008) focused on the characterization of these polymers; later on, attention has been given to the study of chemical and physical factors influencing the light stability of the new binders, especially for artworks exposed to solar radiation (outdoor environment). Additionally, the presence of oxygen was also found to play a major role in polymer stability as it promotes photo-oxidation reactions, such as cross-linking, chain scission, and further oxidation reactions.

Among these polymers, alkyd resins have been widely used in artworks and are the focus of this study. Their first use was documented around the 1940s, and soon they were established as one of the most used materials in modern and contemporary art. They were employed mainly by painters such as Picasso and Pollock, who preferred them to traditional drying oils. During the seventies, they became the prevalent chemical binder in paint artworks (Lake et al., 2004). Chemically, alkyd polymers are composed of oil-modified polyester resins formed from the combination of a polyhydric alcohol (generally glycerol), a polybasic carboxylic acid, and siccative oils or free fatty acids. The oil chain length and weight percent of fatty acids in the alkyd resin molecular structure influence the curing and photodegradation processes (Mallégol et al., 2000a). Photodegradation of alkyd polymers occurs by auto-oxidation of unsaturated bonds of the fatty acid portion forming a cross-linked network.

As a consequence, the newly-formed peroxy and hydroperoxy radicals may react with the alkyd chain leading to further cross-linking and β-scission reactions. Moreover, during auto-oxidation of the oil portion, chemical species such as hydrocarbons, aldehydes, and ketones allow Norrish type I reactions (cleavage or homolysis into free radical intermediates) and chain-scission to take part in the oil degradation. In particular, Norrish type I is the main photodegradation initiation reaction of aromatic polyesters, leading to the formation of free phthalic acid (Lazzari and Chiantore, 1999). Furthermore, hydrogen abstraction (Norrish type II reaction) can take place and products such as ketones, aldehydes, alkene, and carboxylic acids can be formed in the photochemical single state excitation. The abstraction of hydrogen produces alcohols, cyclic structures, carboxylic acids, and vinyl groups. Overall, alkyd resin photo-oxidation results in production of low molecular weight fractions, which either evaporate more easily or remain in the polymeric structure (Lazzari and Chiantore, 1999; Duce et al., 2014). While the several reactions involved in the long-term photo-oxidation have already been extensively studied in previous projects (Pintus et al., 2015; Anghelone et al., 2016), investigating the effect of pigment interaction to the photo stability of alkyd polymers is also fundamental (Mallégol et al., 2000b). In particular, different studies (Rasti and Scott, 1980; Anghelone et al., 2017) show that inorganic pigments can act as retardants or promoters of light-induced aging reactions. To this respect, pigments can be divided into two categories: 1) photo-absorbers, which reduce the impact of light transmitted into the paint layer, and 2) photo-promotors, which increase the photo-oxidation effect with formation of free radicals. Moreover, characteristics of the pigments such as concentration, refractive index (R.I.), and particle size also play a role in the photodegradation process as they can affect the penetration of radiation into the paint layer (Zubielewicz et al., 2011). This study is focused on three inorganic pigments, namely artificial ultramarine blue, hydrated chromium oxide green, and cadmium yellow. These pigments have been used since 1800 as well as in recent contemporary artworks and are still included in formulations of paint tubes. Because of their widespread use among artists, studying their effects on the overall stability of art objects is of high importance (Bevilacqua et al., 2010), not only to prevent aesthetical damage of artworks but also to lower the risk of their physical degradation.

In this work, the surface chemical changes of alkyd paints exposed to short-time artificial sunlight aging were studied. Paint samples were exposed for 168, 336, 504, 672, 840, and 1,008 h (0–6 weeks) to artificial aging, using spectral and intensity parameters comparable to outdoor solar radiation. Several paint samples were prepared by mixing each inorganic pigment (artificial ultramarine blue, hydrated chromium oxide green, and cadmium yellow) with the synthetic binder. Three different pigment/binder (P/BM) ratios were selected (1:2, 1:3, and 1:6) in order to evaluate how the concentration of pigment influences the binder's degradation. The selection of analytical techniques was based on their reciprocal complementarity, which allows supporting the various obtained results and providing new information on the binder's degradation mechanisms. Specifically, 3D Optical Microscopy, Scanning Electron Microscopy (SEM), and Colorimetry allowed studying the morphological and color changes of the paints.

The binder degradation reactions were investigated by Attenuated Total Reflection Infrared Spectroscopy (ATR-FTIR). Firstly, identification of the functional groups found before and after aging was carried out. Subsequently, quantitative analysis was performed to investigate the binder's photodegradation kinetics, taking into consideration the different pigments and P/BM ratios selected. Finally, microscopic images of the paint samples were analyzed using a multivariate approach based on the extraction and analysis of features related to color and texture properties, using Principal Component Analysis (PCA). PCA is a data exploration technique aimed at extracting useful information from a dataset and displaying data structure in a simple and easy-to-interpret manner. Basically, the original dataset is projected into a lower-

TABLE 1 | List of materials analyzed.

Binder	**Chemical composition**		**Commercial name**
Alkyd resin	Polymer oil-modified polyester-resin based on orthophthalic acid and pentaerythritol		Alkyd medium 4 (Lukas®, Germany)
Pigment	**Color index**	**P/BM ratio in weight**	**Chemical composition**
Artificial ultramarine blue	PB29	1:2, 1:3, 1:6	$Na_{6-10}Al_6Si_6O_{24}{\cdot}S_{2-4}$
Hydrated chromium oxide green	PG18	1:2, 1:3, 1:6	$Cr_2O_3{\cdot}2H_2O$
Cadmium yellow	PY37	1:2, 1:3, 1:6	CdS

dimensional space defined by few Principal Components, which are calculated based on data variance. By analysing PCA outcomes it is possible to identify clusters of objects sharing similar properties or relationships among variables (Musumarra and Fichera, 1998). In this study, PCA was applied to the dataset of image features in order to gain an objective and comprehensive overview of the modifications induced by artificial aging on the morphology of the paint layers.

MATERIALS AND METHODS

Sample Preparation

Different samples were prepared by mixing pure Alkyd Medium 4 (Lukas®, Germany) with inorganic pigments (Kremer Pigmente, Germany), i.e., artificial ultramarine blue (PB29), hydrated chromium oxide green (PG18), and cadmium yellow (PY37). A detailed description of the paint samples is shown in **Table 1**. In total, nine samples were prepared. Different P/BM ratios in weight were prepared, depending on the paint's consistency. After a consultation with a paint manufacturer, the P/BM ratios chosen were confirmed as similar to the commercial formulations. The fresh paints were cast on glass slides with a film thickness of 150 μm. The samples were dried at room conditions (ca. 22°C and 30% relative humidity [RH]) for three weeks before starting the artificial aging in the UV chamber. The samples were analyzed every week (max. 1,008 h exposure).

Artificial Aging

The light aging, which simulates natural sunlight, was carried out in a UVACUBE SOL 2/400F UV chamber, produced by Dr. Hönle GmbH UV-Technology, Germany. The emitting radiation was supplied by a Xenon Arc lamp with the possibility to provide radiations between 295 and ~3,000 nm, similar to outdoor solar conditions. Temperature and RH were separately measured in the chamber using the AQL S500 sensor (Aeroqual Limited, New Zealand).

During artificial aging, the chamber temperature was around 38°C, and the RH varied between 10 and 20%. The radiation intensity was measured by using a UV-Meter Basic (Dr. Hönle, Germany). The Xenon lamp reached an approximate value of 170 W/m^2. According to the recent data provided by Central Europe, it is possible to assume that the radiation value obtained is similar to natural aging caused by solar radiation (Šúri et al., 2007). The artificial light exposure of alkyd paints was carried out for 1,008 h in total. Considering that there are around 1,000 h of sunshine per year (global approximation), it is possible to approximate the artificial sun aging of 1,008 h to around one year of natural outdoor sunlight exposure (Šúri et al., 2004). The glass slide was divided into six regions (**Figure 1**) to obtain different aging periods (168–1,008 h) on each paint sample. The regions which were not exposed to artificial light were contact-free covered with a silver-aluminum 100% reflective surface. The reflective cover was moved weekly to obtain the complete 1,008 h aged sample set.

Optical 3-Dimensional Microscope

To monitor the different morphological changes due to artificial light aging, the surface of each colored layer was scanned by the Keyence VHX-6000 microscope (Keyence, Belgium). Three-dimensional optical micrographs and topological images were recorded using a VH-Z100 objective with a zoom lens of 1,000×. For each aging week (from 0 to 1,008 h), surface pictures were acquired. The objective chosen reaches a focus in the range of 100–1,000 μm. The microscope is provided with a LED light source (5,700 K). For the 3D pictures, a magnification of 1,000× was selected, measuring a total area of around 15,376 μm^2. To obtain the 3D depth profile of the surface, the total depth obtained is 10 μm taking every 2 μm a picture (pitch scans). In total, 63 images were acquired using the optical 3D microscope, corresponding to nine samples (three pigments types × 3 P/BM ratios) aged for seven different times from 0 to 1,008 h.

Multivariate Analysis of Microscopic Images

The data obtained by the microscopic images of the paint samples were subjected to multivariate analysis in order to evaluate the degradation effects caused by artificial UV aging. The main focus is put on the feature of the paint samples and to study the influence of pigment type and concentration on such degradation effects. For this aim, a preliminary data dimensionality reduction step was applied to convert each image of the dataset into a feature vector codifying for the useful information related to color and aspect of the analyzed samples. Generally, a data dimensionality reduction procedure is a mandatory step when several images have to be simultaneously analyzed and compared to each other, to gain a general overview of the whole image dataset structure (Calvini et al., 2016). Different methods have been proposed to extract relevant features from images. The most common approach is based on evaluating the pixel distribution of defined color parameters of each image and using the corresponding frequency distribution curves or statistical

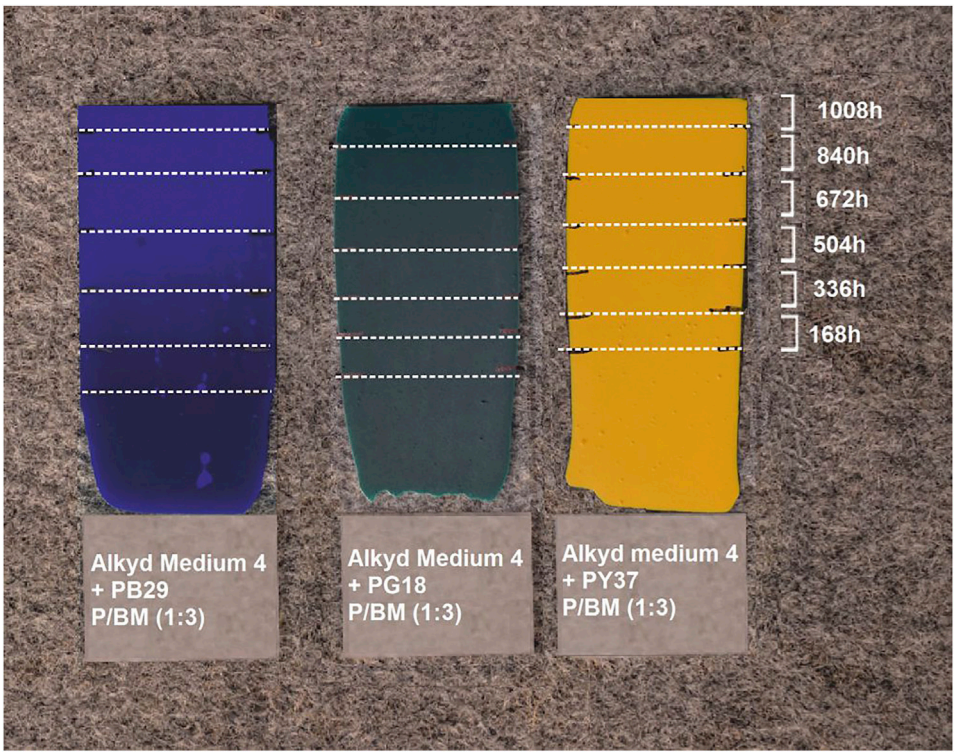

FIGURE 1 | Three paint samples with P/BM ratio 1:3; from left Alkyd Medium 4 + PB29, Alkyd Medium 4 + PG18, Alkyd Medium 4 + PY37. They were exposed to artificial sunlight for 168, 336, 504, 672, 840, and 1,008 h.

parameters calculated from the frequency distribution curves (e.g., mean or standard deviation value) as relevant features (Pereira and Bueno, 2007; Kucheryavski, 2011; Calvini et al., 2020).

Furthermore, in order to fully exploit spatial-related information contained in the images also texture features can be calculated. A widely used image texture analysis approach is the application of Gray Level Co-occurrence Matrices (GLCMs) (Haralick et al., 1973), which records the frequency of occurrence of each possible grey-level pairing of neighboring pixels with a specified spatial arrangement. Given a grey-scale image, four possible orientations of neighboring pixels can be considered to calculate the GLCM: horizontal, right diagonal, vertical, and left diagonal, corresponding to an angle of 0°, 45°, 90°, and 135°, respectively. Then, from each GLCM, it is possible to calculate texture parameters based on first, second, and higher-order statistics and further analyze the obtained texture features using chemometric methods (Malegori et al., 2016; Marschner et al., 2017).

In the present study, a total of 36 features were extracted from each paint sample image. These features include mean, median, and standard deviation and range of red (R), green (G), and blue (B) channels, and of two additional color-related parameters derived from the R, G, and B values: lightness (L), calculated as the sum R, G, and B values, and saturation (S), obtained by converting the RGB color space into the hue-saturation-value (HSV) color space. These features summarise the color-related properties of the images. Furthermore, texture parameters derived from GLCMs of lightness grey-scale images were extracted. Firstly, each RGB microscopic image was converted into the corresponding grey-scale image of lightness obtained by summing the R, G, and B values of each pixel. Then, GLCMs of each lightness grey-scale image were calculated considering all the possible directions of neighboring pixels (0°, 45°, 90°, and 135°). The calculation of the GLCMs was performed considering a distance of 10 pixels and a resolution of 64 grey-scale levels.

Therefore, four GLCMs were obtained from each original microscopic image. Finally, from each GLCM, the following texture parameters were calculated (Fongaro and Kvaal, 2013):

- *Contrast (Con)*, which measures the intensity variations between one pixel and the neighboring pixel; in a constant image, the value of contrast is equal to zero.
- *Correlation (Corr)*, which measures the relation between one pixel and its neighbors, and this correlation can be direct (positive) or indirect (negative).
- *Energy (En)*, which is calculated as the sum of the square of the GLCM elements; it can range between 0 and 1, and for a constant image, its value is equal to 1.
- *Homogeneity (Hom)*, which measures how close the elements of the GLCM are to the diagonal; it can vary between 0 and 1, and its value is equal to 1 for a diagonal GLCM.

The complete list of the 36 color and texture features extracted from each microscopic image is reported in **Supplementary Table S1**. The feature vectors extracted from all the dataset images were collected into a data matrix with 63 rows, corresponding to the number of acquired images, and 36 columns, corresponding to the number of extracted features. Finally, the matrix of image features was analyzed using PCA using autoscale as a data preprocessing method. The extraction of color and texture features from the images was performed using routines written *ad hoc* in MATLAB language (v. 9.8, The MathWorks, Inc., United States) and based on MATLAB Image Processing Toolbox (v. 11.1). At the same time, PCA models were calculated using the PLS_Toolbox software (v. 8.8.1, Eigenvector Research, Inc., United States) running under the MATLAB environment.

Colorimetric Measurements

To obtain colorimetric values between unaged and aged samples, an SPM50 Gretag-Macbeth (XRite, Switzerland) was used. Measurements were carried out by a D65 light source with the 10° Standard Observer, 45°/0° geometry. The spot size measured is around 1 mm. The system was calibrated with an internal white reference. Five spots were measured per exposure and averaged using Microsoft Excel software (Microsoft®, United States). To determine the color changes between unaged and aged samples, CIELAB coordinates (L*, a*, b*) and ΔE^* values were evaluated, according to the Commission Internationale de l'Èclairage 1976 (CIE 1976) (Johnston-Feller, 2001).

Scanning Electron Microscopy

Scanning Electron Microscope (SEM) was employed for investigating the microstructure of paint mixtures, the changes in pigment distribution, and their morphology after aging. Samples were analyzed using a Quanta TM250 FEG Field-Emission Scanning Electron Microscope (Thermo Fisher Scientific, United States), and images were collected under a low vacuum at 20 kV acceleration voltage. Some of the collected images were post-processed using CorelDraw 2018 software, and the pigment particle size was measured using ImageJ v1.52i software.

Attenuated Total Reflection Fourier Transform Infrared Spectroscopy

For the FTIR investigations, a LUMOS FTIR Microscope (Bruker Optics, Germany) in ATR mode with a germanium crystal was employed. The instrument is equipped with a photoconductive cooled MCT detector. Spectra were acquired in a spectral range between 4,000 and 480 cm^{-1}, performing 64 scans at a resolution of 4 cm^{-1}. The resulting spectra were collected and evaluated with the software OPUS® (Bruker Optics, Germany). Five measurement spots were chosen on each unaged and aged paint sample. The spectra were averaged, baseline corrected, and vector normalized. The chemical depth information obtained by the ATR-FTIR measurements, considering the R.I. of the germanium crystal ($n_1 = 4.01$) and the angle of incidence of the IR beam ($\theta = 45°$), in a spectral region between 4,000 and 480 cm^{-1}, is around 0.65 μm.

RESULTS AND DISCUSSION

Optical 3-Dimensional Microscopy Observations

Figure 2 shows how the morphology of the paint layers of the PB29 alkyd samples changes during the light aging process. The surfaces of the unaged samples show an increasingly glossy appearance with increasing polymer content. The morphology of the pores is also different across P/BM ratios. In fact, as the binder content increases, the pore size tends to widen (especially in the P/BM 1:6 sample). After a total of 1,008 h of light aging, different morphological changes are detectable. In the mixture with P/BM 1:6, it is possible to observe that by increasing the UV exposure time, the pores begin to increase in number and to enlarge until the pigment is more visible on the surface. When the binder content is lower (P/BM 1:2), this phenomenon is already observed after 504 h of UV exposure. After 1,008 h of aging, the pigment grains are more visible on the surface and of sharper morphology; moreover, some discoloration can be observed. This aging effect is more noticeable when the P/BM is high (1:2). In *Principal Component Analysis of Features Extracted From Microscopic Images* and *Colorimetric Measurements*, the color changes will be discussed more in detail through multivariate analysis of the microscopic images and colorimetry.

A similar behavior is also observed in the PG18 alkyd samples (**Supplementary Figure S1**). In the 1:6 mixture, after 1,008 h of aging, the surface is less glossy and more porous. As for the blue sample, also in the green 1:2 mixture, the opacity increases over time, probably as a result of the binder's degradation and pigment accumulation on the surface. However, unlike PB29, the PG18 pigment tends to darken, and this effect is particularly visible in the mixture with a high amount of pigment (P/BM 1:2). This morphological and colorimetric behavior is also observable for the PY37 alkyd sample (**Supplementary Figure S2**). However, differently from the two previous paints, the glossy effect is not evident, the pores are much smaller and after aging, they are no longer well-defined. This effect may be due to the granulometry of the yellow pigment, explained in *Colorimetric Measurements* (SEM results).

Principal Component Analysis of Features Extracted From Microscopic Images

Principal Component Analysis Considering All Samples

For the first evaluation of data structure, PCA of the image features matrix was calculated considering all the samples together, and the corresponding results are reported in **Supplementary Figure S3**. PC1 separates PY37 samples from the other two pigments based on color and texture features like homogeneity, energy, and contrast, which have high PC1 loading coefficients in terms of absolute values. In particular, the images of PY37 have higher *Hom* and *En* values, showing a more homogeneous paint layer and the presence of the binder is less evident.

Furthermore, the PC1 and PC3 score plot show that sample PY37 presents a lower variation due to aging, while PB29 paint

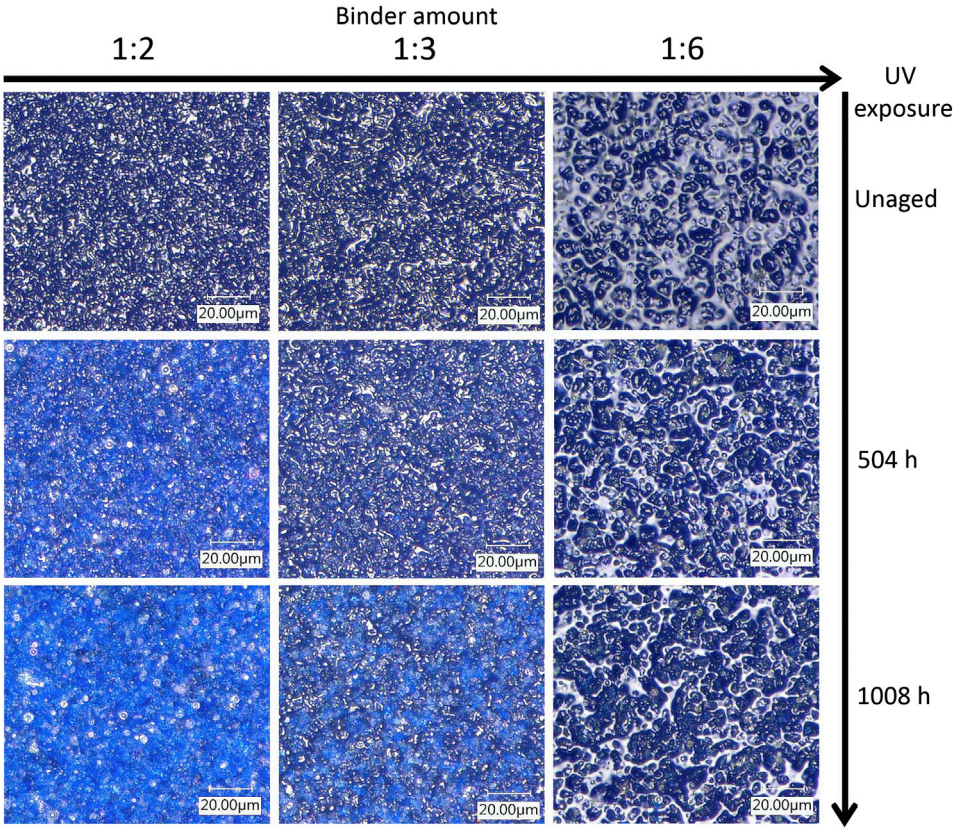

FIGURE 2 | Morphological overview by 3D image (1,000×) of PB29 alkyd samples. From left to right, the samples are displayed according to their different P/BM ratios, whereas the images from top to bottom depict the unaged, 504, and 1,008 h aging.

undergoes higher degradation effects. Similar results are presented in the discussion of the colorimetric measurements (*Colorimetric Measurements*). It has to be noticed that each pigment has a peculiar degradation pattern, and it is difficult to find trends common to all the three pigment types. Besides, it is also possible to observe that there are differences based on the P/BM ratio for each pigment type. Therefore, for a better evaluation of color and texture variations of each pigment due to aging, separate PCA models were calculated for each pigment type.

Principal Component Analysis of PB29 Samples

The PCA model of the samples prepared with PB29 pigment was calculated considering 3 PCs (93.57% of the total variance). The corresponding PC1 and PC2 score and loading plots are reported in **Figures 3A,B**, respectively. The PC1 and PC2 score plot shows that the sample prepared with a P/BM ratio equal to 1:6 presents a lower variation over time due to aging compared to the samples with higher pigment concentrations. In particular, the images of the sample prepared with a P/BM ratio equal to 1:2 have a higher variation in the PC1 and PC2 score plot based on aging time, suggesting that this sample undergoes higher degradation effects. Considering the PC1 and PC2 loading plot, it is possible to observe that the images of the samples with P/BM ratio equal to 1:6 are characterized by low *Hom* and *En* values, while they have high standard deviation values of R, G, S, and L color parameters. These findings are confirmed by observing the microscopic images of PB29 alkyd samples (**Figure 2**), which show that the surface layer of PB29 sample prepared with a P/BM ratio of 1:6 is very heterogeneous due to the high concentration of the binder. Furthermore, PC1 describes the aging pattern common to the samples with P/BM ratio equal to 1:2 and 1:3. For these two concentrations, the images of the unaged samples have negative PC1 values, while increasing the aging time, the images of the samples move toward positive PC1 values. Considering the PC1 loading vector, the image features with positive PC1 values are mean and median values of G, B, S, and L, and homogeneity texture feature. Therefore, with light aging, the PB29 paints with lower binder concentration tend to lighten, and the paint layer seems more homogeneous as the presence of the binder is less evident.

Principal Component Analysis of PG18 Samples

The PCA model of the samples with PG18 was calculated considering 2 PCs (91.80% of the total variance), and **Figures 3C,D** report the corresponding PC1 and PC2 score and loading plots. In this case as well, the sample with a P/BM equal to 1:6 ratio differs from the samples with higher pigment concentration.

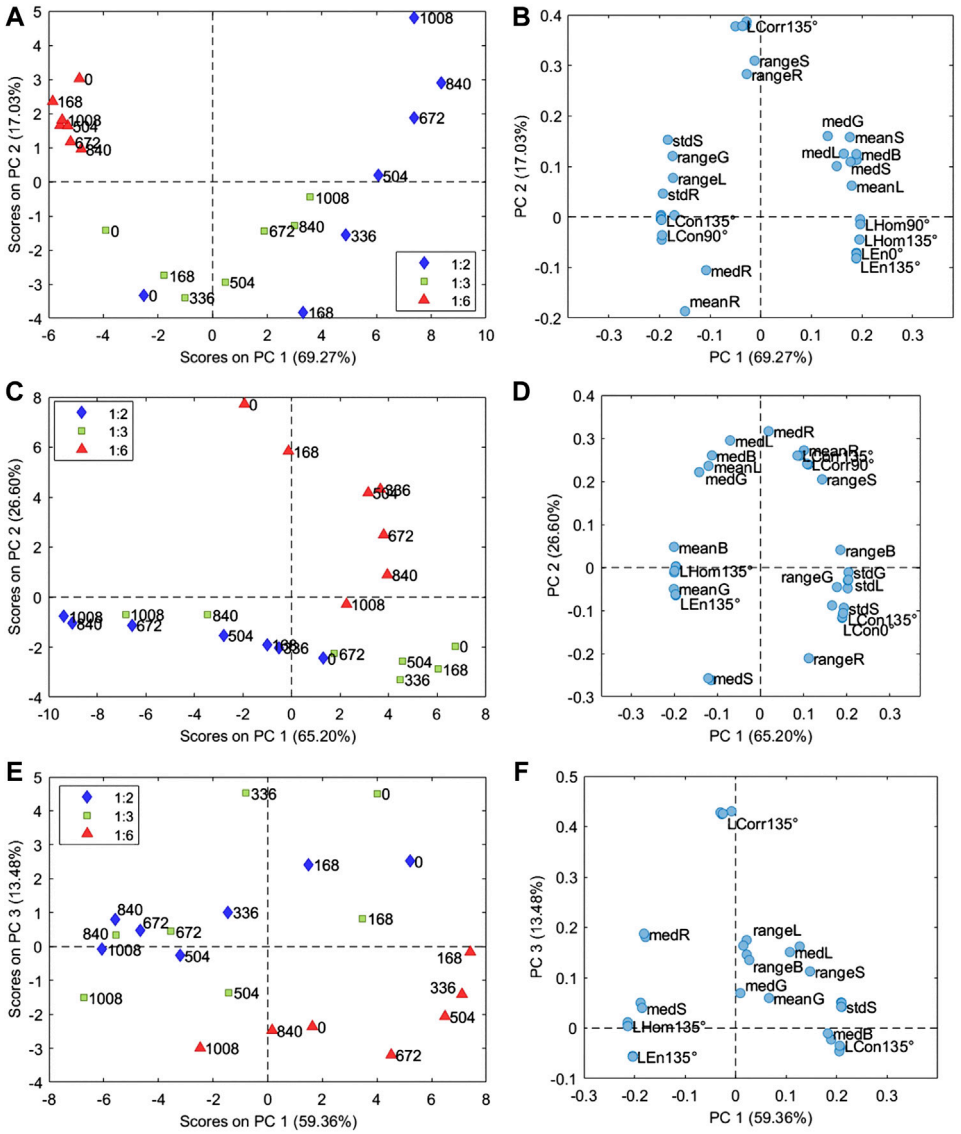

FIGURE 3 | Score and loading plots of the PCA models calculated on the image features matrix (**Supplementary Table S1**) obtained from the microscopic images of samples of alkyd resin mixed with PB29 **(A,B)**, PG18 **(C,D)**, and PY37 **(E,F)**. The samples in the score plot are colored according to the P/BM ratio, while the labels indicate the aging time from 0 to 1,008 h.

Indeed, the variation over time of the 1:6 P/BM ratio sample is mainly described by PC2, while the variation over time of 1:2 and 1:3 P/BM ratio samples is described by PC1. These aging patterns are orthogonal, suggesting that light aging has different effects on the paint layers according to binder concentration. Considering PC1 loadings, it is possible to observe that the images of aged samples with a P/BM ratio of 1:2 and 1:3 exhibit increasing mean and median values of G, B, L, and S parameters while the range and standard deviation of the same color-related parameters tend to decrease. Considering the texture-related parameters, the images of the aged samples have higher *Hom* and *En* values and lower *Con* values. Therefore, during aging, the paint layer of the samples prepared with a lower binder concentration tends to have a more saturated color, and the presence of the binder becomes less visible. As previously mentioned, the aging behavior of the sample with 1:6 P/BM ratio are mainly described by PC2. Comparing PC2 scores and loadings, it is possible to observe that the images of aged samples show increasing range and standard deviation values of R, G, L, and S parameters and also increasing *Con* values. The mean and median values of R, B, and L tend to decrease.

Principal Component Analysis of PY37 Samples

The PCA model of the samples with PY37 was calculated considering 4 PCs (94.74% of the total variance), and the corresponding PC1 and PC3 score and loading plots are reported in **Figures 3E,F**, respectively. PC1 and PC3 score plot shows that samples prepared with the different P/BM

ratios have a similar variation pattern during aging, conversely to what was observed for the paint layers of PB29 and PG18. Indeed, for PY37, the aged samples tend to move toward negative PC1 score values compared to the corresponding unaged samples. Considering PC1 loadings, it is possible to observe that the images of the aged sample have higher *Hom* and *En* values, higher mean and median values of R and S parameters, and lower mean and median values of L. Therefore, PY37 paint layers tend to darken with aging but, at the same time, they present a more saturated color. This behavior is common for all the considered pigment concentrations. Furthermore, PC3 mainly describes the difference between samples with a 1:6 P/BM ratio and samples with the other two pigment concentrations.

Colorimetric Measurements

In **Supplementary Table S2**, the colorimetric results of unaged and 1,008 h UV-aged alkyd paint samples are shown. The results include the colorimetric changes in the values of the lightness/darkness (L*), red/green (a*), yellow/blue (b*), and the total color change from 0 to 1,008 h exposure (ΔE*). The ΔE* values obtained from each colored paint and P/BM ratio were evaluated and compared. It can be observed in **Figure 4** that the most significant color change is recorded for the PB29 paint with P/BM ratio 1:2. This behavior tends to decrease with the increase of the binder amount. A similar trend is detected for PG18 paints but less significant than for the blue paint. Moreover, a relatively significant difference in the shift of the L*, a*, and b* coordinates between the unaged and aged paint samples is observed, confirming the important role that pigments play on the degradation of this binder when exposed to the light. These findings confirm the results obtained from PCA performed on the color and texture features extracted from the microscopic images (*Principal Component Analysis of Features Extracted From Microscopic Images*).

Comparing all the colorimetric values of the three inorganic pigments, the PB29 alkyd paint samples have the most significant shift of a* and b* between unaged and aged samples, showing a strong reduction in red and blue, respectively. The decreasing of a* and b* values and the overall increase of the L* parameter might be due to changes in the surface roughness of the paints (Simonot and Elias, 2003). In fact, after aging, the macroscopic properties of the film change, becoming stiffer and more brittle, probably due to the cross-linking of the residual olefinic unsaturation (Hintze-Brüning, 1993). This phenomenon was also previously confirmed by 3D, SEM microscope, and multivariate results. As reported in the literature (Del Federico et al., 2006; Janssens et al., 2016; René de la Rie et al., 2017), artificial ultramarine blue (PB29) has a significant loss of its blue color when mixed with alkyd resin after light irradiation. This effect is probably due to the chromophoric S-anions release after the opening of the sodalite cages of pigment, leading to the discoloration of the pigment itself. However, in the evaluation of the colorimetric variation percentage of the L* value, the PG18 paint also shows relevant results. In fact, the L*, a*, and b* values of the 1:2 and 1:3 mixtures tend to decrease, indicating a less bright paint layer and a color change toward blue. These results are confirmed by the multivariate analysis of the features extracted from microscopic images, indicating higher saturation values with increasing exposure and increasing pigment amount. This trend is not observable for the 1:6 mixture, as the L* and a* values tend to increase. This behavior could be due to the higher organic component in the paint and its interaction with this particular inorganic pigment. Further studies will be necessary in order to understand these

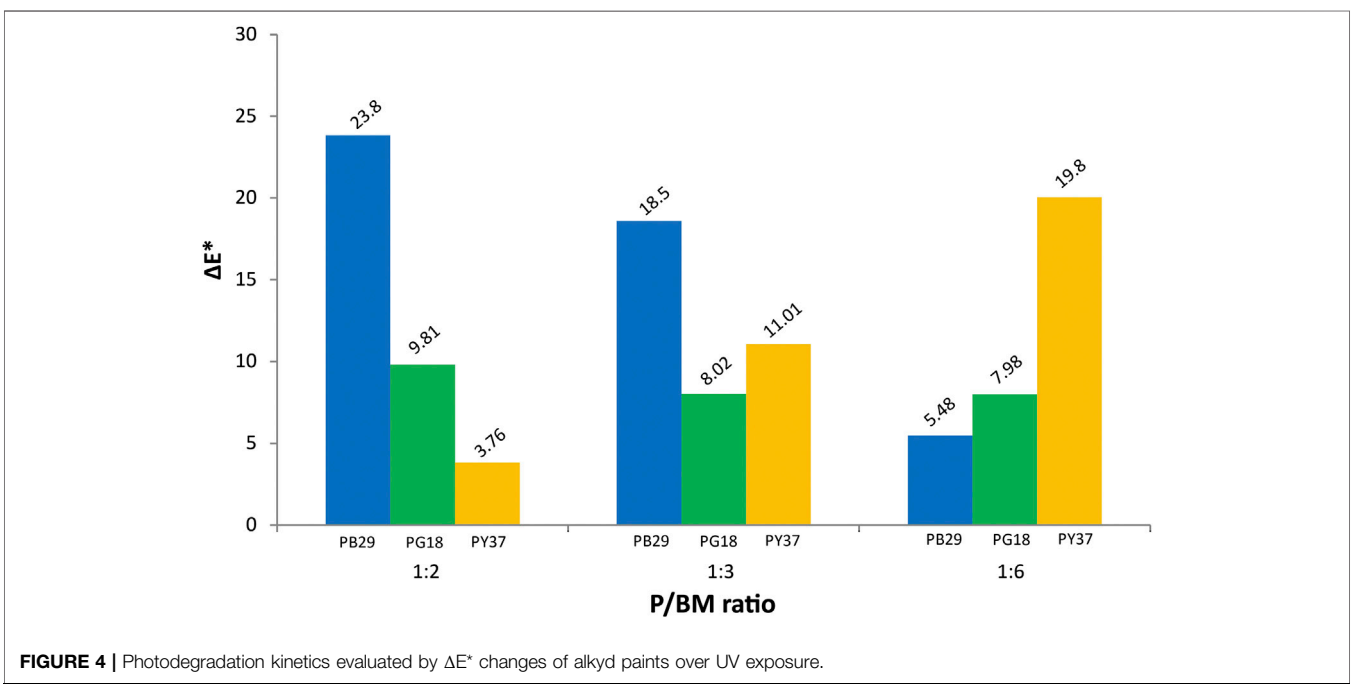

FIGURE 4 | Photodegradation kinetics evaluated by ΔE* changes of alkyd paints over UV exposure.

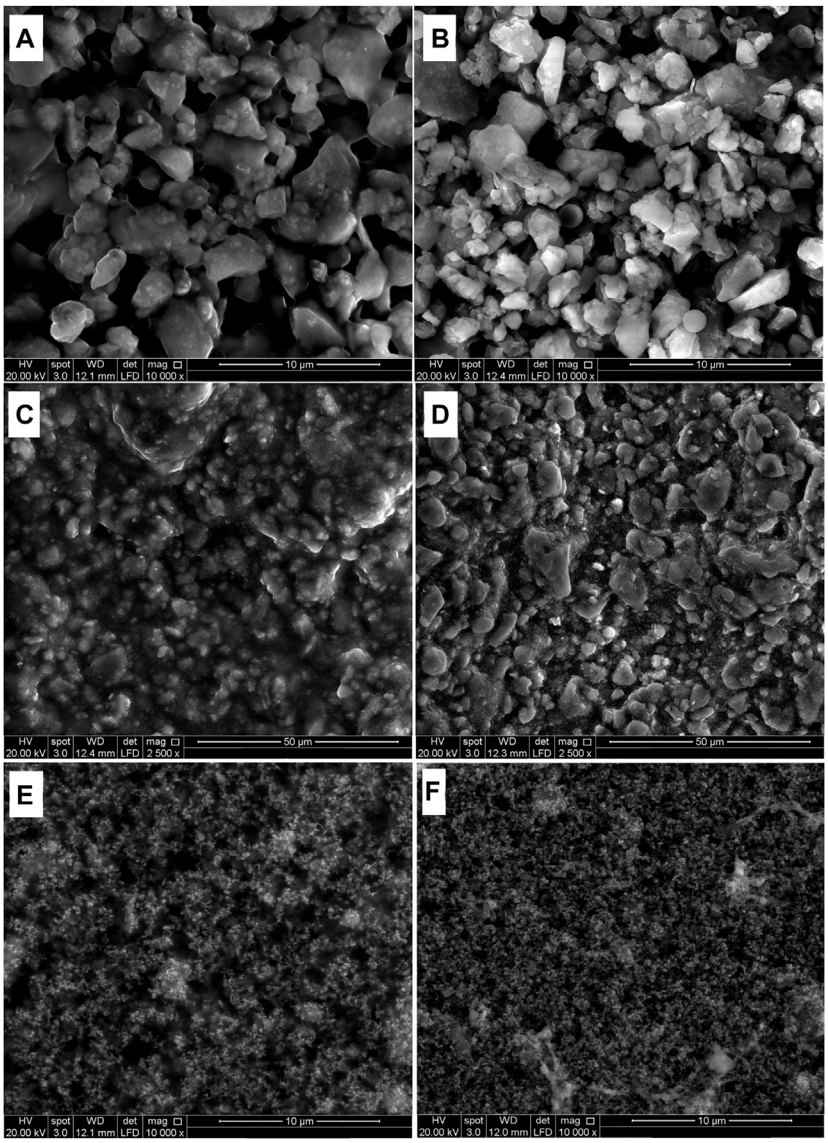

FIGURE 5 | SEM images of alkyd resin mixed with PB29 **(A,B)**, PG18 **(C,D)**, and PY37 **(E,F)**, before aging **(left)** and after 1,008 h aging **(right)**.

effects. As observed in **Figure 4**, the trend of ΔE^* for PY37 paints, according to the different P/BM ratio, is different from the two previous paints. Generally, the L* and a* values do not show significant changes, whereas b* shows the greatest change, especially for the 1:6 mixture. As demonstrated by the ATR-FTIR analysis and the chemometric evaluation, PY37 appears to be the pigment that least affects the degradation of the binder. Therefore this different behavior may be due to the colorimetric change of the organic component, more easily detectable in the PY37 paint than the previous two pigments. Further studies will be needed to better understand these effects. Cadmium yellow (PY37) and hydrated chromium oxide green (PG18) are generally considered as lightfast pigments, therefore the origins of their different color changes are not completely clear (Sward, 1972). During aging, some chemical properties of the paints are deteriorated as the paint film is gradually attacked by oxidizing agents, leading to the breakdown of the polymer molecules into smaller fragments. This phenomenon increases if the pigment concentration is high. During light exposure, the pigment particles placed on the surface will be more subject to photodegradation, leading to the fading or darkening of the color (Turner, 1979). In some cases, the loss of chemical-mechanical properties of the binder mixed with pigment (as for PB29) leads to the highest fragility of the paint on the surface, which becomes almost powdery (chalking).

Scanning Electron Microscopy Results

With SEM analyses it was possible to evaluate the morphological surface changes after artificial light aging considering the different granulometry of the pigments and their amount in

the paint mixtures. Observations of the unaged samples (P/BM 1:2) showed the different morphological features of the pigments. The particle size range of PB29 is around 1–3 μm in diameter, and their shape and average distribution appear irregular and inhomogeneous (**Figure 5A**). A similar observation is shown for PG18, where, however, the grains have a size range from few nm to 1–2 μm (**Figure 5C**). Finally, PY37 is the pigment with the smallest particle size (few nm) and its grains appear to be distributed in agglomerates, making the surface more homogeneous than the other two pigments (**Figure 5E**).

The particle size distribution and R.I. play an important role in the light beam-material interaction and, therefore, on the degradation of the paints. If a paint film contains a pigment with a high R.I., a high fraction of the incident light tends to be bent or refracted at the surface and therefore less likely to interact with and deteriorate the paint materials (Gueli et al., 2016). Observing the R.I. values of the analyzed pigments (Feller, 1986; Roy, 1993; Vahur et al., 2010), PY37 has the highest R.I. (approx. between 2.35 and 2.48), followed by PG18 (1.62–2.12) and by PB29 (1.5). Therefore, light radiation will have a higher impact on the blue paints, followed by green and yellow paint samples. Moreover, the light scattering imparted by diffraction is further affected by the particle size. The smaller the particle size and the higher R.I. are, the more the light beam has a tendency to be scattered (Baker and Lavelle, 1984; Yousif and Haddad, 2013). As previously reported, the granulometric evaluation of the inorganic pigments carried out by SEM measurements confirmed these considerations (Holland and Gagne, 1970; Kremer Pigmente).

However, it is also necessary to consider the influence of the R.I. of the binding medium, the dispersion level of the pigment (i.e., the degree of aggregation of the pigment particles), the proportion of pigment in the vehicle, called pigment volume concentration (PVC), and the thickness of the paint layer (Merwin, 1917). Furthermore, the R.I. is not a constant value, but changes over time according to other factors including the P/BM ratio and the type of pigment employed. In this study, the granulometry of the pigments played a major role in the binder's degradation. In the unaged samples, the alkyd resin is homogeneously dispersed in the film. After aging (**Figures 5B,D,F**), the chemical transformations cause variations in the surface morphology: the binder is no longer visible and the pigment particles are better defined. This behavior is most evident in PB29 and PG18 samples after 504 h of aging. In PY37 paints, the morphology does not change significantly after exposure to aging.

Attenuated Total Reflection Fourier Transform Infrared Spectroscopy Results

For the determination of the photodegradation effects on alkyd paints, the main ATR-FTIR absorption bands of the binder and inorganic pigments were identified according to **Supplementary Table S3** (Vahur et al., 2009; Coccato et al., 2016). Their characterization was based on the analysis of the unaged samples (P/BM 1:2 mixtures presented as reference example), shown in **Figure 6Aa** (for PB29), **Figure 6Ba** (for PG18), and **Figure 6Ca** (for PY37). The unaged spectra of the other mixtures (P/BM 1:3 and 1:6) are not depicted as they show the same absorbance bands but with different intensities, proportional to the binder content. Concerning the alkyd resin, significant contributions of the oil and phthalic components are identified in the polymer. The main absorption bands that identify these two components are related to the C=O stretching vibration at 1,724 cm^{-1}, and the CH_2 and CH_3 stretching and bending (asymmetric and symmetric) at 2,926, 2,854, 1,465, 1,451, and 1,388 cm^{-1}. Additional phthalic bands can be identified mainly by absorption signals corresponding to C=C stretching aromatic ring at 1,600 and 1,588 cm^{-1}, the C-O-C symmetric stretching at 1,260 and 1,114 cm^{-1}, and the aromatic out-of-plane bending at 741 and 709 cm^{-1} (Ellis et al., 1900; Hayes et al., 2014). By comparing the results of the unaged and 1,008 h light aged samples, significant chemical changes on the surface are detected. The results are evaluated according to the type of pigment used, the P/BM ratios, and the contribution of the inorganic components to the degradation process.

Among the PB29 samples aged for 1,008 h, the intensity of the OH stretching band at 3,244 cm^{-1} is the highest in the sample with a high amount of binder (**Figure 6Ad**). Moreover, the (C-H) CH_2 asymmetric and symmetric stretching at 2,926 and 2,854 cm^{-1} disappears. These effects are due to hydrogen abstraction and oxidation of double bonds, respectively (Perrin et al., 2000). A decreasing trend with aging is observed for the carbonyl band at 1,724 cm^{-1}. This band can still be detected after 1,008 h of exposure only in the paint sample with a high amount of binder (P/BM 1:6). Furthermore, in the same sample, the carbonyl band gets broader due to the aging of the oil component in the alkyd binder, which is caused by hydroperoxides and peroxides reactions taking place during photochemical degradation and resulting in oxidation products such as aldehydes, ketones, and carboxylic acids (at 1,735, 1,720, and 1,710 cm^{-1}) (Socrates, 2001). The bands at 1,068 and 984 cm^{-1}, related to the Al,Si-O_4 asymmetric stretching, increase with aging time and the pigment amount in the paint mixture (Bruni et al., 1999). As shown in **Figure 6Ab**, additional pigment bands at 691 and 656 cm^{-1}, related to the Al,Si-O_4 symmetric stretching, are detected. After the maximum exposure time (1,008 h), the intensity of the small band at 470 cm^{-1} has increased. The signal is identified as the O-Si-O bending vibration (Taylor, 1990). The apparent increase in the characteristic PB29 absorption bands is mainly due to the volatilization of the binder on the superficial level of the paint (Mecklenburg et al., 2013; Keune et al., 2016). This chemical-physical phenomenon is very prominent in the alkyd paints due to the oil component, which is very reactive toward the oxidative elements present in the surrounding environment (such as oxygen, sunlight, and O_3), leading to Norrish photo-cleavage reactions and formation of free-radicals, able to make the polymeric films unstable (Berg et al., 1999).

In **Figure 6B**, the ATR-FTIR spectra of alkyd binder in mixture with PG18 in different P/BM ratios (1:2, 1:3, and 1:6) aged for 1,008 h are shown in comparison to the unaged P/BM 1:2 mixture. Overall, all the main absorption bands of the alkyd binder are present (**Supplementary Table S3**), however, after

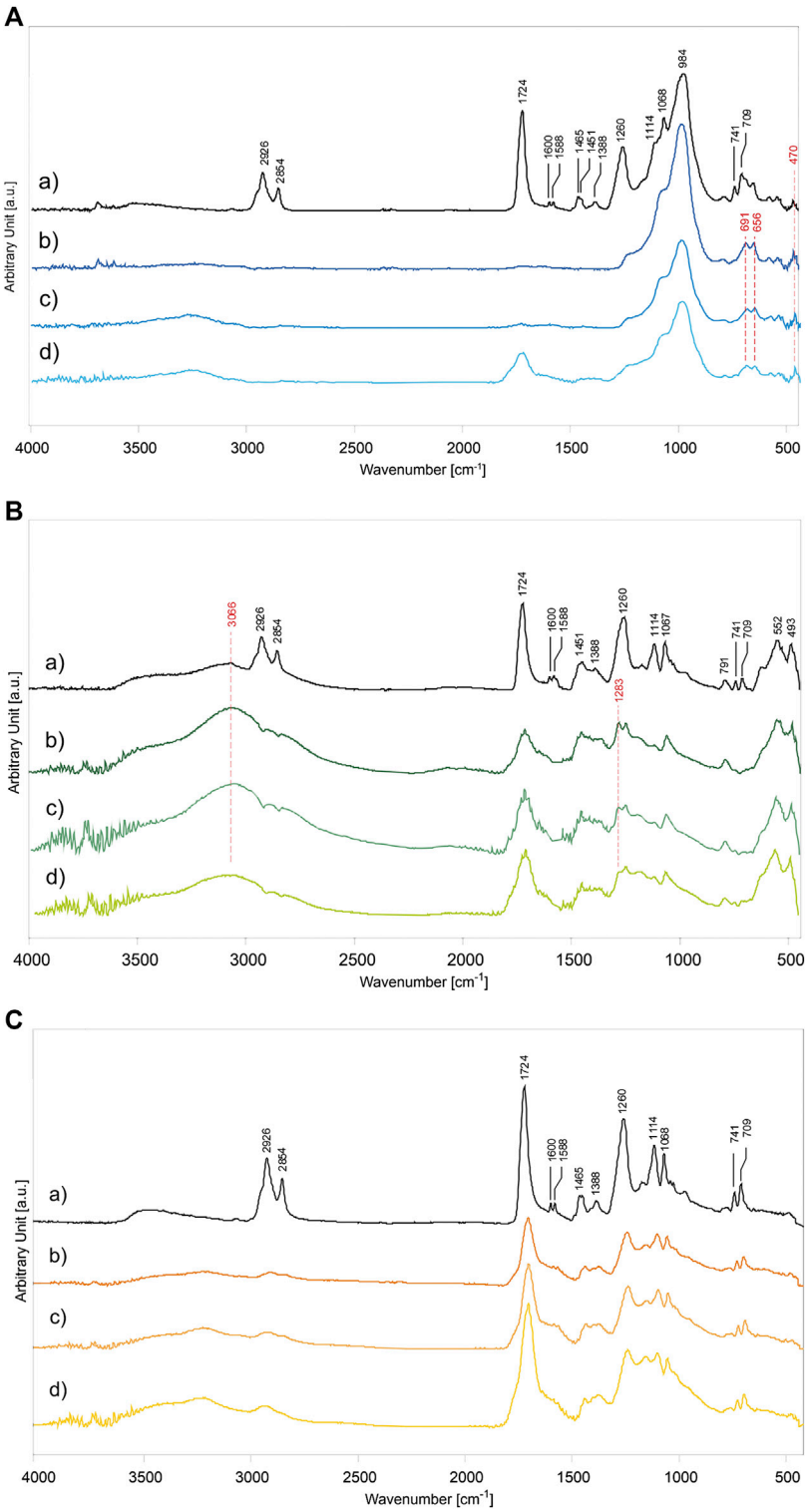

FIGURE 6 | ATR-FTIR spectra of alkyd binder in mixture with inorganic pigments: **(A)** PB29, **(B)** PG18, and **(C)** PY37. The graphs of paint mixtures are, **(a)** unaged P/BM 1:2, and after 1,008 h of UV exposure according to different P/BM ratio: **(b)** 1:2, **(c)** 1:3, and **(d)** 1:6.

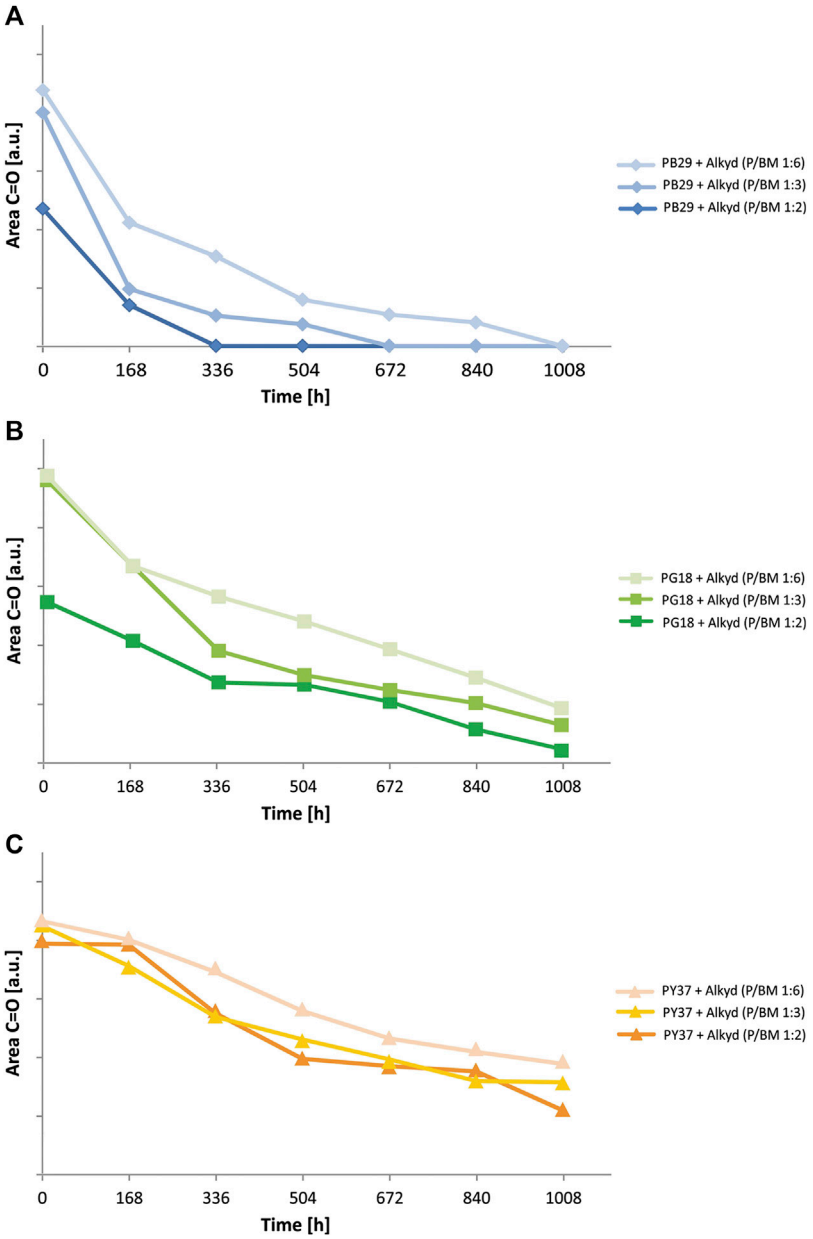

FIGURE 7 | Photodegradation kinetics observed from ATR-FTIR spectra of alkyd paints with **(A)** PB29, **(B)** PG18, and **(C)** PY37, at various P/BM ratios.

light aging, the spectra show a decreasing trend in the intensity of the binder absorption bands, less evident than paints with PB29. In fact, even if the (C-H)CH_2 stretching bands at 2,926 and 2,854 cm^{-1} tend to disappear, the intensity of the C=O band at 1,724 cm^{-1} decreases, the band widens but does not disappear, as seen previously for PB29 mixtures with P/BM 1:2 and 1:3. The decreasing and widening trend of the C=O band may be due to the β-scission and possibly Norrish I reactions of the ester groups in the polyester and oil fractions, leading to the formation of low molecular weight compounds which subsequently volatilize. The formation of the shoulder at about 1,640 cm^{-1} is due to the formation of C=C functional groups resulting from the photodegradation reaction Norrish type II and bond cleavage of the carbonyl compounds subjected to photolysis (Mallégol et al., 2000b; Cakić et al., 2012). Among the PG18 paint samples, the most intense degradation effect is observed in the mixtures with a high amount of pigment (**Figure 6Bb**). Similarly to the PB29 results, the intensities of the PG18 bands at 552 and 493 cm^{-1} (of the oxide part) increase over time due to the degradation and partial evaporation of the binder degradative by-products. Comparing the spectrum of the unaged sample with the aged ones, the intensity of the OH stretching band at

3,066 cm^{-1} increases with the pigment concentration, as opposed to the results obtained in the PB29 mixtures. This is because the same absorption band is also ascribable to the hydrated component of the pigment which, as previously described, increases with aging time. Another absorbance band ascribable to the pigment is registered at 1,283 cm^{-1}. In combination with the band at 1,252 cm^{-1}, its presence can be abscribed to a minor content of chromium borate, a compound used during industrial manufacture of hydrated chromium oxide green pigments (Fitzhugh, 1997; Zambuehl et al., 2009).

In the case of PY37 alkyd paints, the ATR-FTIR spectra present some frequent spectral changes compared with the results obtained for PB29 and PG18 mixtures. The OH stretching band at 3,230 cm^{-1} tends to increase with aging time, similarly to the PB29 samples, and binder concentration. However, observing the spectrum in **Figure 6Cd** (P/BM 1:6), it is noted that the carbonyl group signal at 1,724 cm^{-1} decreases, as observed in PG18 mixtures. Furthermore, this band tends to widen in PY37 samples to a higher extent than in the other two (in PB29 mixture even disappears), suggesting that the PY37 tends to limit the UV radiation-paint layer interaction and therefore the degradation of the binder.

Photodegradation Kinetics

To better understand the influence that each inorganic pigment has on the degradation of the alkyd binder, the kinetic behavior of a specific IR-band of the binder was evaluated. It was studied by integrating the carbonyl group C=O band (at 1,724 cm^{-1}, integration range from 1,800 to 1,640 cm^{-1}) over time. This specific band was selected for several reasons: 1) it shows strong intensity; 2) it is not overlapping with other bands, and 3) it is the most representative band of the binder. In **Figure 7**, the degradation behavior of the different paint mixtures (P/BM 1:2, 1:3, and 1:6) are presented. Generally, the binder's degradation, shown by a decrease of the C=O area values, is observed after 168 h of aging for all three pigment mixtures at P/BM ratios 1:2. In contrast, for those with P/BM ratios 1:6, binder's degradation can be observed approximately after 336 h. However, the kinetic trend changes according to the type of pigment in the mixture. With PB29, the organic binder's degradation is higher than with PG18 and much higher than with PY37. The pigment's contribution to the binder's degradation is important as it can enhance (with PB29 and PG18) or limit (with PY37) the detrimental effects of light irradiation on the degradation process of the binder. At P/BM 1:2, the intensity decrease of the binder's band at 1,724 cm^{-1} is much faster in the blue paint than in the yellow. On the other hand, by increasing the binder amount (P/BM 1:6), its degradation is reduced in all paint mixtures. For a complete kinetic evaluation, the integration of the characteristic bands of inorganic pigments could have potentially confirmed the presented trend. However, this additional evaluation was difficult to carry out as the spectral signal of PY37 cannot be detected in the Mid-IR range due to the detector cut-off. In further studies, the use of other techniques (such as gravimetric analysis) may support the evaluation of the pigments contribution to the different kinetic degradation trends of alkyd paints.

For a more detailed evaluation of the binder degradation rate, according to the pigment and the P/BM ratio used, the different numerical values obtained by integrating the C=O carbonyl band were compared (**Supplementary Table S4**). The area values of each sample for every week (168 h) of aging were determined (Wiesinger et al., 2018). Subsequently, they were obtained by calculating the difference between the area value of the unaged sample and after 1,008 h of exposure, expressed as $\Delta(C{=}O_{unaged/aged})$. The evaluation showed that there is a direct correlation between light exposure time and degradation. In fact, with high values of $\Delta(C{=}O_{unaged/aged})$, the process of photo-oxidation on the surface is more damaging, with the consequent decrease of the C=O band over time. Moreover, the P/BM ratio also plays a role in the degradation effect. In fact, by observing the $\Delta(C{=}O_{unaged/aged})$ values, it is possible to notice that in the samples with a high amount of binder (P/BM 1:6) the photo-oxidative process is reduced. In contrast, in the samples with a high amount of pigment (P/BM 1:2), these values increase, suggesting a more oxidative effect. This trend also changes according to the pigments used. Comparing the three different paints, this difference is more significant in PB29 paints than in PY37. With the increase of the amount of pigment (1:2), these values tend to decrease for mixtures with PB29 and PG18, while for PY37 the trend is similar to those of mixtures with higher concentration of binder. This numerical difference indicates that with the same amount of pigment, the PB29 further facilitates the interaction of light irradiation with the surface of the paint, causing a more rapid decomposition of the alkyd binder.

CONCLUSION

The chemical surface changes on alkyd paints mixed with inorganic pigments and exposed to short-time artificial light aging were documented by optical 3D microscopy and studied by ATR-FTIR, SEM, and colorimetric analysis. To monitor the degradation behavior of each paint sample, three P/BM ratios were selected: 1:2, 1:3, and 1:6. The paint samples were exposed for 1,008 h in total under conditions comparable to outdoor solar conditions. The main degradation reactions that occur in alkyd paints during light aging are:

- Chemical degradation of the alkyd binder is observed after 168 h, shown by an intensity decrease of the functional groups' IR bands (**Supplementary Table S3**) of the alkyd resin over time. This trend is most evident in the mixtures with the blue pigment PB29, followed by PG18, whereas in those with the yellow pigment PY37, the binder is more stable.
- As a consequence of the binder's decomposition, the pigments' IR absorbance bands show an increase during light exposure in all paint samples.
- The kinetic evaluation of ΔE^* shows that the PB29 alkyd mixture (P/BM 1:2) undergoes the highest color change, followed by PY37 and PG18.
- Morphological changes of the paint surfaces are visible by 3D microscopy and SEM. Upon aging, the samples' surfaces appear more rigid and opaque, as well as less bright and stiffer in paints

with P/BM 1:2. Generally, when the pigment content is low, the degradation behavior is reduced due to light irradiation.
- Finally, PCA was applied to study the microscopic images of the paint samples, considering the color and texture changes after aging. This application was useful for studying degradation effects, focusing on the objective information related to the modifications induced by artificial UV aging based on the impact of pigments and P/BM ratio. This approach can be further implemented for quantitative evaluation of aging time for diagnostic purposes.

In conclusion, the paint samples exposed to artificial light aging show degradation processes that vary according to the binder, the inorganic pigment, and the P/BM ratio employed. The presence of pigments can enhance several photo-oxidative effects on the binder; indeed, PB29 causes higher degradation than PY37 and PG18. Additionally, degradation of the binder increases with pigment concentration. With this study, it has been demonstrated that the use of non-invasive analytical techniques, kinetic evaluation of their results, and the combination of analytical data with chemometric methods have high potential in the identification of paint components of complex artworks and in obtaining in-depth chemical information to be complemented with historical-artistic knowledge (Rosi et al., 2020).

DATA AVAILABILITY STATEMENT

The original contributions presented in the study are included in the article/**Supplementary Material**, further inquiries can be directed to the corresponding author.

AUTHOR CONTRIBUTIONS

LP developed the multi-analytical approach based on scientific investigations on alkyd paints. She prepared the paint samples and personally performed the acquisition and interpretation of data; finally, she wrote the article. RC carried out the multivariate analysis based on 3D microscopic images and wrote the corresponding discussion part in the article. RW supervised the acquisition and interpretation of data, contributing to the revision of this article. JW performed the analysis by SEM, helping during the result evaluation. MS supervised the research work and performed scientific editing of the text. All authors read and approved the final manuscript.

ACKNOWLEDGMENTS

We gratefully acknowledge Cecilia Pesce (Department of Architecture and Built Environment, Faculty of Engineering and Environment, Northumbria University, Newcastle upon Tyne, United Kingdom) for helping with the English corrections. This manuscript has been released as a pre-print at the platform Research Square, section Materials Chemistry (Pagnin et al., 2020). The authors acknowledge their respective institutions.

SUPPLEMENTARY MATERIAL

The Supplementary Material for this article can be found online at: https://www.frontiersin.org/articles/10.3389/fmats.2020.600887/full#supplementary-material.

REFERENCES

Anghelone, M., Jembrih-Simbürger, D., Pintus, V., and Schreiner, M. (2017). Photostability and influence of phthalocyanine pigments on the photodegradation of acrylic paints under accelerated solar radiation. *Polym. Degrad. Stabil.* 146, 13–23. doi:10.1016/j.polymdegradstab.2017.09.013

Anghelone, M., Jembrih-Simbürger, D., and Schreiner, M. (2016). Influence of phthalocyanine pigments on the photo-degradation of alkyd artists' paints under different conditions of artificial solar radiation. *Polym. Degrad. Stabil.* 134, 157–168. doi:10.1016/j.polymdegradstab.2016.10.007

Baker, E. T., and Lavelle, J. W. (1984). The effect of particle size on the light attenuation coefficient of natural suspensions. *J. Geophys. Res.* 89, 8197–8203. doi:10.1029/jc089ic05p08197

Berg, J. D. J., Berg, K-J., and Boon, J. J. (1999). "Chemical changes in curing and ageing oil paints," in 12th triennial meeting Lyon, Lyon, France, August 29–September 3, 1999 (ICOM-CC ICOM Committee for Conservation), Vol. 1, 248–253.

Bevilacqua, N., Borgioli, L., and Adrover Gracia, I. (2010). *I pigmenti nell´arte dalla preistoria alla rivoluzione industriale*. Villatora, Italy: Il prato.

Bruni, S., Cariati, F., Casadio, F., and Toniolo, L. (1999). Spectrochemical characterization by micro-FTIR spectroscopy of blue pigments in different polychrome works of art. *Vib. Spectrosc.* 20, 15–25. doi:10.1016/s0924-2031(98)00096-4

Cakić, S. M., Ristić, I. S., Vladislav, J. M., Stamenković, J. V., and Stojiljković, D. T. (2012). IR-change and colour changes of long-oil air drying alkyd paints as a result of UV irradiation. *Prog. Org. Coat.* 73, 401–408. doi:10.1016/j.porgcoat.2010.12.002

Calvini, R., Foca, G., and Ulrici, A. (2016). Data dimensionality reduction and data fusion for fast characterization of green coffee samples using hyperspectral sensors. *Anal. Bioanal. Chem.* 408 (26), 7351–7366. doi:10.1007/s00216-016-9713-7

Calvini, R., Orlandi, G., Foca, G., and Ulrici, A. (2020). Colourgrams GUI: a graphical user-friendly interface for the analysis of large datasets of RGB images. *Chemometr. Intell. Lab. Syst.* 196, 103915. doi:10.1016/j.chemolab.2019.103915

Chiantore, O., and Rava, A. (2005). *Conserving contemporary art: issues, methods, materials, and research*. Los Angeles, CA: Getty Conservation Institute.

Coccato, A., Bersani, D., Coudray, A., Sanyova, J., Moens, L., and Vandenabeele, P. (2016). Raman spectroscopy of green minerals and reaction products with an application in Cultural Heritage research. *J. Raman Spectrosc.* 47, 1429–1443. doi:10.1002/jrs.4956

Del Federico, E., Shöfberger, W., Schelvis, J., Kapetanaki, S., Tyne, L., and Jerschow, A. (2006). Insight into framework destruction in ultramarine pigments. *Inorg. Chem.* 45, 1270–1276. doi:10.1021/ic050903z

Duce, C., Della Porta, V., Tiné, M. R., Spepi, A., Ghezzi, L., Colombini, M. P., et al. (2014). FTIR study of ageing of fast drying oil colour (FDOC) alkyd paint replicas. *Spectrochim. Acta Part A Mol. Biomol. Spectrosc.* 130, 214–221. doi:10.1016/j.saa.2014.03.123

Ellis, G., Claybourn, M., and Richards, S. E. (1900). The application of Fourier Transform Raman spectroscopy to the study of paint system. *Spectrochim. Acta Part A Mol. Biomol. Spectrosc.* 46, 227–241. doi:10.1016/0584-8539(90)80092-D

Feller, R. L. (1986). *Artists' pigments, a handbook of their history and characteristics*. Washington, DC: National Gallery of Art Washington.

Fitzhugh, E. W. (1997). *Artists' pigments, a handbook of their history and characteristics*. Washington, DC: National Gallery of Art Washington.

Fongaro, L., and Kvaal, K. (2013). Surface texture characterization of an Italian pasta by means of univariate and multivariate feature extraction from their texture images. *Food Res. Int.* 51 (2), 693–705. doi:10.1016/j.foodres.2013.01.044

Gueli, A. M., Bonfiglio, G., Pasquale, S., and Troja, S. O. (2016). Effect of particle size on pigments colour. *Color Res. Appl.* 42, 236–243. doi:10.1002/col.22062

Haralick, R. M., Shanmugam, K., and Dinstein, I. H. (1973). Textural features for image classification. *IEEE Trans. Syst., Man, Cybern.* 3 (6), 610–621. doi:10.1109/tsmc.1973.4309314

Hayes, P. A., Vahur, S., and Leito, I. (2014). ATR-FTIR spectroscopy and quantitative multivariate analysis of paints and coating materials. *Spectrochim. Acta Part A Mol. Biomol. Spectrosc.* 133, 207–213. doi:10.1016/j.saa.2014.05.058

Hintze-Brüning, H. (1993). Utilization of vegetable oils in coatings. *Ind. Crops Prod.* 1, 89–99. doi:10.1016/0926-6690(92)90005-G

Holland, A. C., and Gagne, G. (1970). The scattering of polarized light by polydisperse systems of irregular particles. *Appl. Opt.* 9, 1113–1121. doi:10.1364/ao.9.001113

Janssens, K., Van der Snickt, G., Vanmeert, F., Legrand, S., Nuyts, G., Alfeld, M., et al. (2016). Non-invasive and non-destructive examination of artistic pigments, paints, and paintings by means of X-ray methods. *Top. Curr. Chem.* 374, 81. doi:10.1007/s41061-016-0079-2

Johnston-Feller, R. (2001). *Color science in the examination of museum objects: nondestructive procedures*. Los Angeles, CA: The Getty Conservation Institute.

Keune, K., Mass, J., Mehta, A., Church, J., and Meire, F. (2016). Analytical imaging studies of the migration of degraded orpiment, realgar, and emerald green pigments in historic paintings and related conservation issues. *Herit Sci*. 4, 10. doi:10.1186/s40494-016-0078-1

Kremer Pigmente. Catalogue online. Avialable at: http//www.kremer-pigmente.com (January 20, 2020).

Kucheryavski, S. (2011). Extracting useful information from images. *Chemometr. Intell. Lab. Syst.* 108 (1), 2–12. doi:10.1016/j.chemolab.201va0.12.002

Lake, S., Ordonez, E., and Schilling, M. (2004). A technical investigation of paints used by Jackson Pollock in his drip or poured paintings. *Stud Conser*. 49 (2), 137–141. doi:10.1179/sic.2004.49.s2.030

Lazzari, M., and Chiantore, O. (1999). Drying and oxidative degradation of linseed oil. *Polym. Degrad. Stabil.* 65, 303–313. doi:10.1016/s0141-3910(99)00020-8

Learner, T. (2008). *Modern paints uncovered*. Los Angeles, CA: Getty Conservation Institute.

Malegori, C., Franzetti, L., Guidetti, R., Casiraghi, E., and Rossi, R. (2016). GLCM, an image analysis technique for early detection of biofilm. *J. Food Eng.* 185, 48–55. doi:10.1016/j.jfoodeng.2016.04.001

Mallégol, J., Gardette, J.-L., and Lemaire, J. (2000a). Long-term behavior of oil-based varnishes and paints. Photo- and thermooxidation of cured linseed oil. *J. Am. Oil Chem. Soc.* 77, 257–263. doi:10.1007/s11746-000-0042-4

Mallégol, J., Lemaire, J., and Gardette, J.-L. (2000b). Drier influence on the curing of linseed oil. *Prog. Org. Coating* 39, 107–113. doi:10.1016/s0300-9440(00)00126-0

Marschner, C. B., Kokla, M., Amigo, J. M., Rozanski, E. A., Wiinberg, B., and McEvoy, F. J. (2017). Texture analysis of pulmonary parenchymateous changes related to pulmonary thromboembolism in dogs–a novel approach using quantitative methods. *BMC Vet. Res.* 13 (1), 219. doi:10.1186/s12917-017-1117-1

Mecklenburg, M. F., Tumosa, C. S., and Vicenzi, E. P. (2013). "The influence of pigments and ion migration on the durability of drying oil and alkyd paints," in New insights into the cleaning of paintings: proceedings from the cleaning 2010 international conference, Universidad Politecnica de Valencia and Museum Conservation Institute (Washington, DC: Smithsonian Institution Scholarly Press), 59–67.

Merwin, H. E. (1917). Optical Properties and Theory of Color of Pigments and Paints. *Proc. Amer. Soc. Test. Mater*. XVII, 494–530.

Musumarra, G., and Fichera, M. (1998). Chemometrics and cultural heritage. *Chemometr. Intell. Lab. Syst.* 44, 363–372. doi:10.1016/s0169-7439(98)00069-0

Pagnin, L., Wiesinger, R., and Schreiner, M. (2020). *Photodegradation kinetics of alkyd paints: the influence of varying amounts of inorganic pigments on the stability of the synthetic binder*. Durham, NC: Research Square. . Available at: https://www.researchsquare.com/article/rs-13183/v1 (Accessed June 15, 2020).

Pereira, F. M. V., and Bueno, M. I. M. S. (2007). Image evaluation with chemometric strategies for quality control of paints. *Anal. Chim. Acta*. 588 (2), 184–191. doi:10.1016/j.aca.2007.02.009

Perrin, F. X., Irigoyen, M., Aragon, E., and Vernet, J. L. (2000). Artificial aging of acrylurethane and alkyd paints: a micro-ATR spectroscopic study. *Polym. Degrad. Stabil.* 70, 469–475. doi:10.1016/s0141-3910(00)00143-9

Pintus, V., Wei, S., and Schreiner, M. (2015). Accelerated UV ageing studies of acrylic, alkyd, and polyvinyl acetate paints: influence of inorganic pigments. *Microchem. J.* 124, 949–961. doi:10.1016/j.microc.2015.07.009

Rabek, J. F. (1995). *Polymer photodegradation, mechanisms and experimental methods*. New York, NY: Wiley.

Rasti, F., and Scott, G. (1980). The effects of some common pigments on the photo-oxidation of linseed oil-based paint media. *Stud. Conserv*. 25, 145–156. doi:10.1179/sic.1980.25.4.145

René de la Rie, E., Michelin, A., Ngako, M., Del Federico, E., and Del Grosso, C. (2017). Photo-catalytic degradation of binding media of ultramarine blue containing paint layers: a new perspective on the phenomenon of "ultramarine disease" in paintings. *Polym. Degrad. Stabil.* 144, 43–52. doi:10.1016/j.polymdegradstab.2017.08.002

Rosi, F., Miliani, C., Delaney, J., Dooley, K., Stringari, L., Subelyte, G., et al. (2020). "Chapter I. Jackson pollock's drip paintings: tracing the introduction of alkyds through non-invasive analysis of mid-1940s paintings," in *Science and art*. London, UK: Royal Society of Chemistry, 1–18. doi:10.1039/9781788016384-00001

Rosu, D., and Visakh, P. M. (2016). *Photochemical behaviour of multicomponent polymeric-based materials*. New York, NY: Springer.

Roy, A. (1993). *Artists' pigments, a handbook of their history and characteristics*. Washington, DC: National Gallery of Art Washington.

Simonot, L., and Elias, M. (2003). Color change due to surface state modification. *Color Res. Appl.* 28, 45–49. doi:10.1002/col.10113

Socrates, G. (2001). *Infrared and Raman characteristic group frequencies*. New York, NY: Wiley.

Šúri, M., Huld, T. A., and Dunlop, E. D. (2004). PV-GIS: a web based solar radiation database for the calculation of PV potential in Europe. *Int. J. Sustain. Energy* 24, 55–67. doi:1080/14786450512331329556

Šúri, M., Huld, T. A., Dunlop, E. D., and Ossenbrink, H. A. (2007). Potential of solar electricity generation in the European Union member states and candidate countries. *Sol. Energy*. 81, 1295–1305. doi:10.1016/j.solener.2006.12.007

Sward, G. G. (1972). *Paint testing manual: physical and chemical examination of paints, varnishes, lacquers and colors*. West Conshohocken, PA: ASTM International.

Taylor, W. R. (1990). Application of infrared spectroscopy to studies of silicate glass structure: examples from the melilite glasses and the systems Na_2O-SiO_2 and Na_2O-Al_2O_3-SiO_2. *J. Earth Syst. Sci.* 99, 99–117. doi:10.1007/bf02871899

Turner, G. P. A. (1979). *Introduction to paint chemistry and principle of paint technology*. New York, NY: Chapman and Hall.

Vahur, S., Knuutinen, U., and Leito, I. (2009). ATR-FT-IR spectroscopy in the region of 500-230cm−1 for identification of inorganic red pigments. *Spectrochim. Acta Part A Mol. Biomol. Spectrosc.* 73, 764–771. doi:10.1016/j.saa.2009.03.027

Vahur, S., Teearu, A., and Leito, I. (2010). ATR-FT-IR spectroscopy in the region of 550-230cm−1 for identification of inorganic pigments. *Spectrochim. Acta Part A Mol. Biomol. Spectrosc.* 75, 1061–1072. doi:10.1016/j.saa.2009.12.056

Wiesinger, R., Pagnin, L., Anghelone, M., Moretto, L. M., Orsega, E. F., and Schreiner, M. (2018). Pigment and binder concentrations in modern paint samples determined by IR and Raman spectroscopy. *Angew. Chem. Int. Ed.* 57, 7401–7407. doi:10.1002/anie.201713413

Yousif, E., and Haddad, R. (2013). Photodegradation and photostabilization of polymers, especially polystyrene: review. *SpringerPlus*. 2, 398. doi:10.1186/2193-1801-2-398

Zambuehl, S., Scherrer, N. C., Berger, A., and Eggenberger, U. (2009). Early Viridian pigment composition characterization of a (hydrated) chromium oxide borate pigment. *Stud. Conserv.* 54, 149–159. doi:10.1179/sic.2009.54.3.149

Zubielewicz, M., Kamińska-Tarnawska, E., Ślusarczyk, A., and Langer, E. (2011). Prediction of heat build-up of solar reflecting coatings based on physico-chemical properties of complex inorganic colour pigments (CICPs). *Prog. Org. Coating* 72, 65–72. doi:10.1016/j.porgcoat.2011.02.008

Conflict of Interest: The authors declare that the research was conducted in the absence of any commercial or financial relationships that could be construed as a potential conflict of interest.